POSIVA 97-10

Application of surface complexation modelling:

Nickel sorption on quartz, manganese oxide, kaolinite and goethite, and thorium on silica

Markus Olin
Jarmo Lehikoinen
VTT Chemical Technology

December 1997

POSIVA OY
Mikonkatu 15 A, FIN-00100 HELSINKI, FINLAND
Phone (09) 2280 30 (nat.), (+358-9-) 2280 30 (int.)
Fax (09) 2280 3719 (nat.), (+358-9-) 2280 3719 (int.)

POSIVA 97-10

Application of surface complexation modelling:

Nickel sorption on quartz, manganese oxide, kaolinite and goethite, and thorium on silica

Markus Olin
Jarmo Lehikoinen
VTT Chemical Technology

December 1997

POSIVA OY
Mikonkatu 15 A, FIN-00100 HELSINKI, FINLAND
Phone (09) 2280 30 (nat.), (+358-9-) 2280 30 (int.)
Fax (09) 2280 3719 (nat.), (+358-9-) 2280 3719 (int.)

ISBN 951-652-035-9
ISSN 1239-3096

Posiva-raportti – Posiva report

Posiva Oy
Mikonkatu 15 A, FIN-00100 HELSINKI, FINLAND
Puh. (09) 2280 30 – Int. Tel. +358 9 2280 30

Raportin tunnus – Report code
POSIVA 97-10

Julkaisuaika – Date
December 1997

Tekijä(t) – Author(s)

Markus Olin,
Jarmo Lehikoinen,
VTT Chemical Technology

Toimeksiantaja(t) – Commissioned by

Posiva Oy

Nimeke – Title

APPLICATION OF SURFACE COMPLEXATION MODELLING: NICKEL SORPTION ON QUARTZ, MANGANESE OXIDE, KAOLINITE AND GOETHITE, AND THORIUM ON SILICA

Tiivistelmä – Abstract

This study is a follow-up to a previous modelling task on mechanistic sorption. The experimental work has been carried out at the Laboratory of Radiochemistry, University of Helsinki (HYRL), and the sorption modelling was performed using the HYDRAQL code. Parameters taken from the open literature were employed in the modelling phase. The thermodynamic data for aqueous solutions were extracted from the EQ3/6 database and subsequently modified for HYDRAQL where necessary.

The experimental data were obtained from five different experiments, four of which concerned the adsorption of nickel. The first experimental system was a mixture of Nilsiä quartz and manganese dioxide. In the second experiment, quartz was equilibrated with a fresh and saline groundwater simulant instead of an electrolyte solution. The third and fourth experiments dealt with nickel adsorption from an electrolyte solution onto goethite and kaolinite surfaces respectively. In the fifth experiment, adsorption of thorium onto a quartz surface was investigated.

The modelling of the first experimental system was successful provided an updated set of sorption parameters for both quartz and manganese dioxide was adopted.

For simulated groundwaters, the pre-modelling correctly predicted the experimentally observed lower adsorption of nickel in the saline simulant than in the fresh one.

The sorption of nickel onto a goethite surface over the entire pH range was successfully predicted in the pre-modelling and no further modelling effort was needed.

The sorption of nickel onto a kaolinite surface was considerably more difficult to model than the previous system. The pre-modelling results provided a poor fit to experimental results at lower ionic strengths (0.001 M, 0.01 M). The phenomenon is similar to that observed earlier for quartz. It was not possible to improve the fit in the final modelling using the existing sorption data.

The experiments on the adsorption of thorium on quartz were of a preliminary nature. The predictions from pre-modelling were fair enough and could be slightly improved in the final modelling.

Avainsanat - Keywords
sorption, surface complexation, modelling, nickel, thorium, quartz, manganese oxide, kaolinite, goethite

ISBN
ISBN 951-652-035-9

ISSN
ISSN 1239-3096

Sivumäärä – Number of pages
24

Kieli – Language
English

VTT KEMIANTEKNIIKKA
Ympäristötekniikka

LOPPURAPORTTI Dnro 168-97/KET36

28.10.1997 1 (1)

Posiva Oy
Margit Snellman
Mikonkatu 15 A

00100 HELSINKI

Tilauksenne numero 9513/96/LPN

PINTAKOMPLEKSAATIOMALLIEN SOVELTAMINEN NIKKELIN SORPTIOON OKSIDIPINNOILLE

Loppuraportti tutkimuksesta pintakompleksaatiomallien soveltaminen nikkelin sorptioon oksidipinnoille.

Markus Olin
Erikoistutkija

LIITE 1 kpl loppuraportteja (toimitettu myös sähköisesti)

VTT KEMIANTEKNIIKKA
Ympäristötekniikka
PL 1403
02044 VTT

Katuosoite:
Betonimiehenkuja 5
02150 Espoo

Puh.vaihde (09) 4561
Telekopio (09) 456 7022
Http://www.vtt.fi/

Posiva-raportti – Posiva report

Posiva Oy
Mikonkatu 15 A, FIN-00100 HELSINKI, FINLAND
Puh. (09) 2280 30 – Int. Tel. +358 9 2280 30

Raportin tunnus – Report code
POSIVA 97-10

Julkaisuaika – Date
Joulukuu 1997

Tekijä(t) – Author(s)

Markus Olin,
Jarmo Lehikoinen,
VTT Kemiantekniikka

Toimeksiantaja(t) – Commissioned by

Posiva Oy

Nimeke – Title

PINTAKOMPLEKSAATIOMALLINNUKSEN SOVELTAMINEN: NIKKELIN SORPTIO KVARTSIIN, MANGAANIDIOKSIDIIN, KAOLINIITTIIN JA GÖTIITTIIN SEKÄ THORIUMIN SORPTIO KVARTSIIN

Tiivistelmä – Abstract

Työ on jatkoa aiemmin suoritetulle mekanistiselle sorptiomallinnukselle ja edellisen vaiheen tapaan kaikki aiheeseen liittyvä kokeellinen työ on tehty Helsingin yliopiston radiokemian laboratoriossa (HYRL). Kaikki sorptiomallinnukset on tehty HYDRAQL-mallilla. Mallinnuksessa on yleensä käytetty kirjallisuudesta otettuja sorptioparametreja. Varsinainen vesiliuosten termodynaaminen data on saatu EQ3/6:n termodynaamisesta tietokannasta, joka on muokattu tarvittavin osin HYDRAQLille sopivaan muotoon.

Mallinnettava kokeellinen aineisto koostuu viidestä erityyppisestä kokeesta, joista kaikissa yhtä lukuunottamatta oli kyse nikkelin sorptiosta. Ensimmäisessä koesarjassa Nilsiän kvartsin sekaan lisättiin mangaanidioksidia. Toinen koesarja tehtiin kvartsilla käyttäen elektrolyyttiliuoksen sijaan makeaa ja suolaista simuloitua pohjavettä. Kolmas ja neljäs koesarja käsitteli nikkelin sorptiota elektrolyyttiliuoksesta götiitti- ja kaoliniittipinnoille. Viides koesarja koostui thoriumin sorptiosta kvartsipinnalle.

Kvartsin ja mangaanidioksidin sekoituksella tehtyjen uusien sorptiokokeiden mallinnus kyettiin tekemään menestyksellä, kun käytettiin uutta parametrijoukkoa sekä kvartsille että mangaanille.

Simuloidun pohjaveden tapauksessa esimallinnuksessa kyettiin ennustamaan havaittu, makeaa vettä selvästi alempi, nikkelin sorptio suolaisemmassa vesityypissä.

Nikkelin sorptio götiittipinnalle kyettiin ennustamaan jo esimallinnusvaiheessa niin hyvin, ettei lisämallinnusta tarvittu.

Nikkelin sorptio kaoliniittipinnalle oli edellistä vaikeampi mallintaa ja esimallinnuksen tulokset eivät vastanneet kovin hyvin koetuloksia alhaisessa (0.001 M, 0.01 M) ionivahvuudessa. Ilmiö on samantapainen kuin aiemmin kvartsilla tehdyissä kokeissa havaittu. Epäyhteensopivuutta ei kyetty poistamaan tarkennetulla mallinnuksella olemassaolevalla sorptiodatalla.

Kokeet thoriumin sorptiosta kvartsipinnalle olivat alustavia, mutta esimallinnustuloksia voi pitää kohtalaisina ja niitä kyettiin vielä lopullisessa mallinnuksessa hiukan parantamaan.

Avainsanat - Keywords
sorptio, pintakompleksaatio, mallinnus, nikkeli, thorium, kvartsi, mangaanidioksidi, kaoliniitti, götiitti

ISBN	ISSN
ISBN 951-652-035-9	ISSN 1239-3096
Sivumäärä – Number of pages: 24	Kieli – Language: Englanti

CONTENTS

PREFACE

This study has been carried out by VTT Chemical Technology for Posiva Oy. The contact persons in this study were Lauri Pöllänen and Margit Snellman from Posiva, and Markus Olin from VTT. The experimental part of the study, carried out by Laboratory of Radiochemistry, University of Helsinki (HYRL), has been published as a separate report (Puukko and Hakanen, 1997).

1 INTRODUCTION

Sorption reactions – attachment of aqueous species to solid surfaces – are important retardation mechanisms for radionuclides released from final repositories of spent nuclear fuel. In safety assessment studies and in most transport models, sorption is modelled by means of the linear sorption isotherm, using K_d-coefficients (sorption distribution factor). The K_d-approach has disadvantages, one of the biggest being that K_d is not constant, but depends on factors like pH or ionic strength. The aim of mechanistic modelling is to understand the system well enough to determine which parameters are the key characteristics of the system. Some of these parameters may be measurable, e.g., mineral composition and surface area, while some of them stem from previous experiments as fitted parameters, e.g., binding constants. The binding constant is the thermodynamic substitute for K_d, which is a phenomenological quantity.

Mechanistic sorption models are straightforward to implement into aqueous speciation and solubility models, because surface complexation reactions are mathematically equal to aqueous reactions. Therefore, this approach offers a method for extending standard hydrochemical models to take account of sorption. Surface complexation modelling needs only a few parameters for a given system, and once these are known it is, in principle, possible to model adsorption over wide pH and concentration ranges. However, the application of surface complexation modelling to natural systems is considerably more difficult than that to simple and well-defined laboratory experiments. There are several reasons for this, including lack of consistent data, difficulties in distinguishing between alternative complexation models, difficulties in measuring surface site densities on the adsorbents, and difficulties in summing up the behaviour of the natural mixture system (not only one pure mineral but a mixture of clays, oxides, etc.). Furthermore, natural systems also contain compounds other than (hydr)oxides, which are more difficult to model: for example, clay minerals, micas, zeolites, and most manganese oxides (Kent *et al.*, 1986).

In this report, surface complexation modelling is applied to nickel, Ni(II), sorption on quartz (SiO_2), goethite (α-FeOOH), hydrous ferric oxides (HFO, e.g. $Fe_2O_3 \cdot H_2O$), manganese oxide (MnO_2) and kaolinite ($Al_2Si_2O_5(OH)_4$), and thorium, Th(IV), sorption on quartz. The modelled experiments (Puukko and Hakanen, 1997) were carried out at the Laboratory of Radiochemistry, University of Helsinki (HYRL), and they were preceded by a preliminary modelling task (see section 2.2 in this report)

All the sorption modelling has been performed using the HYDRAQL model (Papelis *et al.*, 1988), which is especially suited to surface complexation modelling of sorption. Some background electrolyte calculations were repeated with EQ6 in order to see differences between the computer models. To make this comparison easier, the HYDRAQL database was modified so as to make the data needed in this report the same for both models. The other reason for the modification is that the data in HYDRAQL are more or less undocumented.

2 THERMODYNAMIC DATA AND PRE-MODELLING RESULTS

Modelling-data consist of two parts: general parameters, such as thermodynamic equilibrium constants, and system-specific parameters, such as measured quantities of electrolytes. The values for these parameters are given below followed by a brief discussion on the quality of a given value. Before carrying out the experiments, a pre-modelling step was taken and the results from this stage are compared with experimental values.

2.1 AQUEOUS SPECIES AND MINERALS

2.1.1 Solutions

Varying the Na-OH-NO_3 composition controlled the ionic strength and pH in the modelled experimental arrangement. Three ionic strengths, I, were typically used: 0.001 mol/L, 0.01 mol/L and 0.1 mol/L. The modelled pH-values were varied between 2 and 10. The HYDRAQL model controls only the proton activity during pH-stepping and, therefore, all other concentrations (sodium and nitrate) are kept at constant values during the stepping. This kind of approach may occasionally cause high electrical imbalance, which is easy to perceive from HYDRAQL's output files, however.

In some experiments, two types of synthetic groundwater were used. The first one was a fresh-water simulant, while the other simulated the saline groundwater at Olkiluoto from borehole OL-KR1 at a depth of 613–618 m. Compositions of both waters are given in Table 1. Only the main components are included.

All activity coefficients were calculated by the Davies equation (Davies, 1962), which is suitable for the ionic strengths used (I < 0.3–1 mol/L). In all calculations, the log fugacity of CO_2-gas was fixed at -3.5, which corresponds to ambient conditions. The temperature was set at 25 °C.

Table 1. *The compositions of the simulated fresh and saline groundwaters in mmol/L (Puukko and Hakanen, 1997).*

Solute	Fresh simulant	Saline simulant
K^+	0.501	22.5
Na^+	11.1	171
Ca^{2+}	2.24	79.7
Mg^{2+}	0.889	2.0
Cl^-	6.79	356
SO_4^{2-}	0.5	-
HCO_3^-	10.1	
Br^-	-	1.2
Ionic strength, I	21.5	440
pH	≈8.1	≈7

Table 2. *Electrolyte aqueous species and minerals (EQ3/6 DATA0.COM.R2, Wolery, 1992).*

Code	Reaction	log K
Aqueous species		
1000	$Ca^{2+} + CO_3^{2-} = CaCO_3(aq)$	3.33
1010	$Ca^{2+} + CO_3^{2-} + H^+ = CaHCO_3^+$	11.38
1020	$Ca^{2+} + SO_4^{2-} = CaSO_4(aq)$	2.11
1030	$Ca^{2+} + Cl^- = CaCl^+$	-0.7
1350	$Ca^{2+} + H_2O = CaOH^+ + H^+$	-12.85
1360	$Mg^{2+} + CO_3^{2-} = MgCO_3(aq)$	2.98
1370	$Mg^{2+} + CO_3^{2-} + H^+ = MgHCO_3^+$	11.37
1380	$Mg^{2+} + SO_4^{2-} = MgSO_4(aq)$	2.41
1385	$Mg^{2+} + Cl^- = MgCl^+$	-0.13
1740	$4Mg^{2+} + 4H_2O = Mg_4(OH)_4^{4+} + 4H^+$	-39.8
1960	$K^+ + SO_4^{2-} = KSO_4^-$	0.880
1962	$K^+ + Cl^- = KCl(aq)$	-1.49
2000	$Na^+ + CO_3^{2-} = NaCO_3^-$	0.516
2005	$Na^+ + CO_3^{2-} + H^+ = NaHCO_3$	10.48
2010	$Na^+ + SO_4^{2-} = NaSO_4^-$	0.820
12530	$H^+ + CO_3^{2-} = HCO_3^-$	10.33
12540	$2H^+ + CO_3^{2-} = H_2O + CO_2(aq)$	16.67
12550	$H^+ + SO_4^{2-} = HSO_4^-$	1.98
13595	$H_2O = H^+ + OH^-$	-13.99
Minerals		
20000	$Ca^{2+} + CO_3^{2-} = CaCO_3$ (Calcite)	8.48
20002	$Ca^{2+} + CO_3^{2-} = CaCO_3$ (Aragonite)	8.34
20010	$Ca^{2+} + SO_4^{2-} + 2H_2O = CaSO_4{:}2H_2O$ (Gypsum)	4.48
20012	$Ca^{2+} + SO_4^{2-} = CaSO_4$ (Anhydrite)	4.31
20130	$Ca^{2+} + 2H_2O = Ca(OH)_2 + 2H^+$ (Portlandite)	-22.6
20140	$Mg^{2+} + CO_3^{2-} + 3H_2O = MgCO_3{:}3H_2O$ (Nesquehonite)	5.33
20142	$Mg^{2+} + CO_3^{2-} + 5H_2O = MgCO_3{:}5H_2O$ (Lansfordite)	5.49
20144	$2Mg^{2+} + CO_3^{2-} + 5H_2O = Mg_2CO_3(OH)_2{:}3H_2O + 2H^+$ (Artinite)	-9.32
20145	$Ca^{2+} + Mg^{2+} + 2CO_3^{2-} = CaMg(CO_3)_2$ (Dolomite)	16.6
20146	$Mg^{2+} + SO_4^{2-} + 7H_2O = MgSO_4{:}7H_2O$ (Epsomite)	1.96
20200	$Mg^{2+} + 2H_2O = Mg(OH)_2 + 2H^+$ (Brucite)	-16.3
Gaseous species		
25000	$2H^+ + CO_3^{2-} = H_2O + CO_2(gas)$	18.14

The user of the HYDRAQL must form the thermodynamic database himself, because no audited data are available in HYDRAQL-format. We have modified the HYDRAQL database (seen in Table 2) from EQ3/6-database DATA0.COM.R2 (Wolery, 1992), which we mainly use in our EQ3/6 modelling work.

2.1.2 Nickel

Thermodynamic data for nickel in aqueous systems are somewhat uncertain; carbonate species especially are either included or rejected altogether. In this report, the pertinent reactions and thermodynamic constants for nickel, shown in Table 3, are used (EQ3/6 DATA0.COM.R2, Wolery, 1992). In all experimentation, a trace amount of nickel was used. This ensures that saturation of surface adsorption sites with the metal only will not take place.

Table 3. *Nickel aqueous species and minerals.*

HYDRAQL code	Reaction	log K
Aqueous species		
6775	$Ni^{2+} + SO_4^{2-} = NiSO_4(aq)$	2.13
6780	$Ni^{2+} + Cl^- = NiCl^+$	-1.00
6800	$Ni^{2+} + Br^- = NiBr^+$	-0.37
6960	$Ni^{2+} + NO_3^- = NiNO_3^+$	0.40
6961	$Ni^{2+} + 2NO_3^- = Ni(NO_3)_2$	0.19
7591	$Ni^{2+} + 2H_2O = Ni(OH)_2 + 2H^+$	-20.0
7592	$Ni^{2+} + 3H_2O = Ni(OH)_3^- + 3H^+$	-31.0
7594	$2Ni^{2+} + H_2O = Ni_2OH^{3+} + H^+$	-10.7
7595	$4Ni^{2+} + 4H_2O = Ni_4(OH)_4^{4+} + 4H^+$	-27.7
Minerals		
20710	$Ni^{2+} + CO_3^{2-} = NiCO_3$	6.82
20750	$Ni^{2+} + 2H_2O = Ni(OH)_2 + 2H^+$	-12.8

2.1.3 Thorium

The thermodynamic data for thorium are given in Table 4 (EQ3/6 DATA0.COM.R2, Wolery, 1992).

2.2 SURFACE REACTIONS

2.2.1 Quartz

Two types of quartz, Min-U-Sil 5 (MUS) and Nilsiä (NLS), were used in HYRL's experiments (Puukko and Hakanen, 1997). The specific surface area of different quartz samples varied from 0.7 to 6.2 m^2/g. For the modelling, the values given by

Puukko and Hakanen (1997) were adopted: 3.96 m^2/g for MUS and 1.33 m^2/g for NLS. The site density was assumed to be 6 nm^{-2} or 10.0 $\mu mol/m^2$, which is slightly higher than the literature value of 8.3 $\mu mol/m^2$. Values for the site density and binding constants are coupled as their product is used by the model; only in the case when the sorption sites all become occupied is there a difference between the higher site density and higher binding constant. In HYRL's experiments, the quartz concentration was 60 g/L (42–372 m^2/L), which corresponds to 0.42–3.7 mmol/L.

When the triple-layer model is used, the capacitances of the inner and outer layers are needed. For the outer-layer capacitance, a "standard" value of 0.2 F/m^2 is used. For quartz, the inner-layer capacitance varies between 0.9 and 1.25 F/m^2, depending on the literature source. In this report, the latter value, 1.25 F/m^2, was adopted for all computations. In the diffuse-layer model, the model itself defines the capacitance.

The characteristics and surface reactions for quartz are given in Tables 5 and 6, respectively. The last inner-sphere reaction in Table 6 is one chosen by Östhols (1995) and conforms to the diffuse double-layer model (DDLM). It should be noted that although Östhols uses two sorption sites, the stoichiometry for sorption sites in the mass action equation is one and, consequently, the sorption site concentration should be divided by two.

Table 4. *Thorium: aqueous species and minerals.*

HYDRAQL code	Reaction	log K
Aqueous species		
11870	$Th^{4+} + SO_4^{2-} = ThSO_4^{+2}$	5.31
11880	$Th^{4+} + 2SO_4^{2-} = Th(SO_4)_2(aq)$	9.62
11890	$Th^{4+} + Cl^- = ThCl^{+3}$	0.954
11891	$Th^{4+} + 2Cl^- = ThCl_2^{+2}$	0.676
11892	$Th^{4+} + 3Cl^- = ThCl_3^+$	1.50
11893	$Th^{4+} + 4Cl^- = ThCl_4(aq)$	1.07
12090	$Th^{4+} + H_2O = ThOH^{3+} + H^+$	-3.89
12091	$Th^{4+} + 2H_2O = Th(OH)_2^{2+} + 2H^+$	-7.11
12092	$Th^{4+} + 3H_2O = Th(OH)_3^+ + 3H^+$	-11.9
12093	$Th^{4+} + 4H_2O = Th(OH)_4 + 4H^+$	-16.0
12094	$2Th^{4+} + 2H_2O = Th_2(OH)_2^{6+} + 2H^+$	-6.46
12095	$4Th^{4+} + 8H_2O = Th_4(OH)_8^{8+} + 8H^+$	-21.8
12096	$6Th^{4+} + 15H_2O = Th_6(OH)_{15}^{9+} + 15H^+$	-37.7
Minerals		
21380	$Th^{4+} + 4H_2O = Th(OH)_4 + 4H^+$	-9.65
21381	$Th^{4+} + 2H_2O = ThO_2 + 4H^+$ (Thorianite)	-1.86
21382	$Th^{4+} + 4NO_3^- + 5H_2O = ThO(NO_3)_4{:}5H_2O$	-1.78

2.2.2 Manganese oxide and hydrous ferric oxide (HFO)

In our previous work (Olin, 1995), it became apparent that quartz alone is not capable of explaining all the measurements and, therefore, two additional surface types, manganese oxide and hydrous ferric oxides, were also introduced. These surfaces are modelled in the same way as quartz and all the parameters needed for them are shown in Tables 5 and 6. For manganese oxide some of the data have been changed compared to the previous work (Olin, 1995). The HYDRAQL model can handle one or two surfaces together, but not three, and therefore all three surfaces were not simultaneously present in any calculation.

Table 5. *Characteristics of quartz, manganese dioxide and hydrous ferric oxide (HFO) (Puukko et al., 1995; Dzombak and Morel, 1990; Balistrieri and Murray, 1982; Kent et al., 1986). For comparison data for goethite (Puukko and Hakanen, 1997; Coughlin and Stone, 1995) are also shown.*

Parameter	Quartz	MnO_2	HFO	Goethite
Specific surface area, m^2/g	0.7-6.2	300	600	35.6
N_s, site density, nm^{-2}	6	18	3	7
N_s, site density, $\mu mol/m^2$	10	30	5	12
Sites per mass, $\mu mol/g$	8	9 000	3 000	410
Inner-layer capacitance, F/m^2	1.25	2.40	1.40	1.10
Outer-layer capacitance, F/m^2	0.2	0.2	0.2	0.2

Table 6. *Surface reactions (TLM) of quartz, manganese dioxide, hydrous ferric oxide (HFO) and goethite, for comparison (Puukko et al., 1995; Dzombak and Morel, 1990; Balistrieri and Murray, 1982, Kent et al., 1986, Coughlin and Stone, 1995; Östhols, 1995; Zachara et al., 1990; Leckie, 1995; Payne and Waite, 1991).*

Reaction	Quartz	MnO_2	HFO	Goethite
Inner-sphere				
$SOH = SO^- + H^+$	-7.8	-4.2	-10.7	-11.1
$SOH + H^+ = SOH_2^+$	-	-	5.1	5.8
$SOH + Ni^{2+} = SONi^+ + H^+$	-	-	-	-0.7
$2SOH + Th^{4+} = (SO)_2\,Th^{2+} + 2H^+$	-1.9	-	-	-
Outer-sphere				
$SOH + Na^+ = SO^- - Na^+ + H^+$	-5.7	-3.3	-9.0	-8.8
$SOH + NO_3^- + H^+ = SOH_2^+ - NO_3^-$	-	-	-	7.6
$SOH + H^+ + Cl^- = SOH_2^+ - Cl^-$	-	-	6.9	-
$SOH + Ni^{2+} = SO^- - Ni^{2+} + H^+$	-5.5	-2.5	-2.0	-
$SOH + Ni^{2+} + H_2O =$ $SO^- - Ni(OH)^+ + 2H^+$	-12.4	-	-	-
$SOH + K^+ = SO^- - K^+ + H^+$	-5.7	-	-9.0	-
$SOH + Ca^{2+} = SO^- - Ca^{2+} + H^+$	-7.32	-	-6.3	-
$SOH + Mg^{2+} = SO^- - Mg^{2+} + H^+$	-7.32	-	-6.3	-

2.2.3 Kaolinite

The physical parameters of the adsorbent and surface chemical reactions for nickel adsorption on kaolinite are presented in Tables 7 and 8 respectively. The surface complexation model used here to quantify Ni(II) adsorption was the constant capacitance model (CCM). In Table 8, X represents an amount of solid bearing one equivalent of intrinsic negative charge. In addition to these cation-exchange sites, kaolinite particle edges carry ionizable tetrahedrally and octahedrally bound Si- and Al-hydroxyl sites respectively. Within the framework of the CCM, all surface complexes having Si or Al as their central atom assume inner-sphere coordination.

2.2.4 Goethite

The physical parameters of the adsorbent as well as surface chemical reactions for nickel adsorption on goethite are as shown in Tables 5 and 6. The surface complexation model selected to quantify Ni(II) adsorption was the triple-layer model (TLM). The concentration of the solid was 1 g/L (Puukko and Hakanen, 1997).

Table 7. *Characteristics of kaolinite (KGa-1).*

Parameter	Value
BET surface area, S_{BET}	11.38 m^2/g[†]
Edge surface area, S	6.15 m^2/g (= $0.54S_{BET}$)[‡]
Capacitance, C	1.06 F/m^2[§]
Cation-exchange capacity, CEC	10 μmol/g[¶]
Tetrahedral site density, $N_{s,SiOH}$	4.53 $\mu mol/m^2$[£]
Octahedral site density, $N_{s,AlOH}$	9.07 $\mu mol/m^2$[£]
Concentration of solid, a	20 g/L[†]

† Puukko and Hakanen (1997).

‡ Xie and Walther (1992). This is the (assumed) reactive area for surface hydroxyl groups.

§ Goldberg (1993).

¶ Due to isomorphous substitution in the lattice (in particular Al(III) for Si(IV)) or 2:1 phyllosilicate contaminants, or both (estimated value). Ideally, the kaolinite crystal carries no permanent, pH-independent, charge originating from isomorphous substitution.

£ White and Zelazny (1988).

Table 8. Nickel surface chemical equilibria on kaolinite.

Surface reaction	log K
$Na^+ + X^- = NaX$	20.0†
$H^+ + X^- = HX$	22.9‡
$Ni^{2+} + 2X^- = NiX_2$	40.8§
$SiOH = SiO^- + H^+$	-6.53¶
$SiOH + Ni^{2+} = SiONi^+ + H^+$	-6.2£
$2SiOH + Ni^{2+} = (SiO)_2 Ni^+ + 2H^+$	-11.9£
$AlOH + H^+ = AlOH_2^+$	7.2¶
$AlOH = AlO^- + H^+$	-9.5¶
$AlOH + Ni^{2+} = AlONi^+ + H^+$	-3.7£
$2AlOH + Ni^{2+} = (AlO)_2 Ni^+ + 2H^+$	-10.7£

† By assumption.
‡ Schindler *et al.* (1987).
§ Calculated from the Na-K exchange data of Ewin *et al.* (1981) and the K-Ni exchange data of Bansal (1982).
¶ Schindler and Sposito (1991).
£ Calculated from the correlation between surface complexation and complex formation in solution (Schindler, 1991; Schindler and Sposito, 1991).

2.3 PRE-MODELLING AND EXPERIMENTAL RESULTS

2.3.1 Nickel on a mixture of quartz and MnO_2

The experimental results from nickel sorption on a mixture of quartz and MnO_2 are shown in Figure 1. No pre-modelling was carried out for this system. The purpose of the experiment was to test the hypothesis of MnO_2 impurities being the reason for high sorption at low pH and ionic strength.

2.3.2 Nickel on quartz in synthetic groundwater

The sorption results from experiments carried out at HYRL (Puukko and Hakanen, 1997) coincide with the predicted curve only occasionally (Figures 2 and 3). In accordance with model predictions, sorption in the saline water is considerably less than in the fresh water.

2.3.3 Nickel on kaolinite

Nickel sorption on kaolinite was studied at three ionic strengths (0.001 M, 0.01 M and 0.1 M), and the experimental and pre-modelling results for these systems are shown in Figures 4, 5 and 6.

2.3.4 Nickel on goethite

The experimental and pre-modelling results for sorption of nickel on goethite are shown in Figure 7.

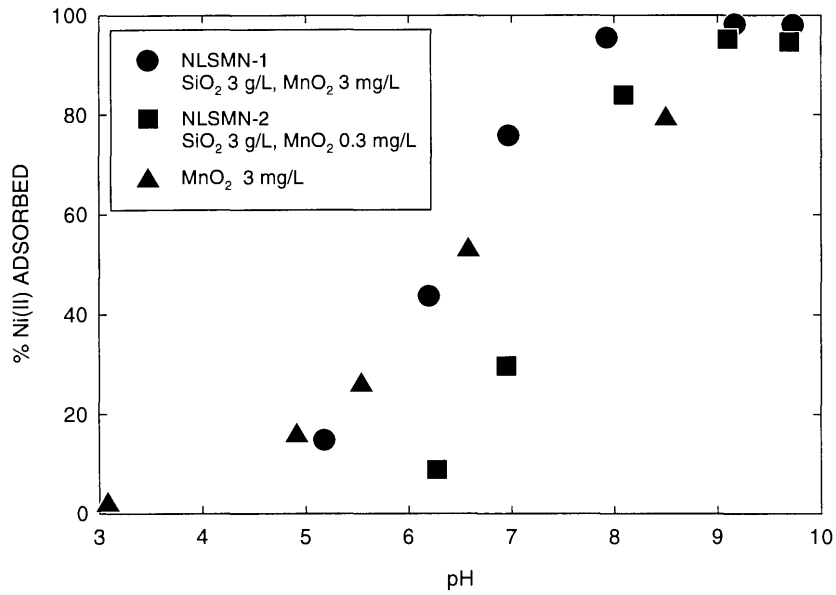

Figure 1. *Experimental Ni(II) sorption on a mixture of quartz and MnO_2 in 0.001 M $NaNO_3$ (Puukko and Hakanen, 1997).*

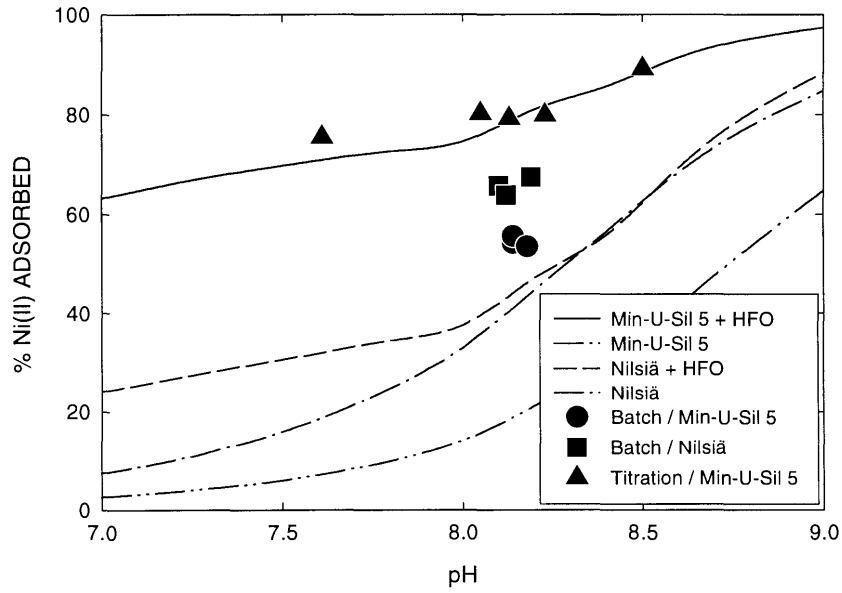

Figure 2. *Predicted (curves) vs. experimental (symbols) Ni(II) sorption on quartz in the fresh groundwater simulant. For experimental data, consult Puukko and Hakanen (1997).*

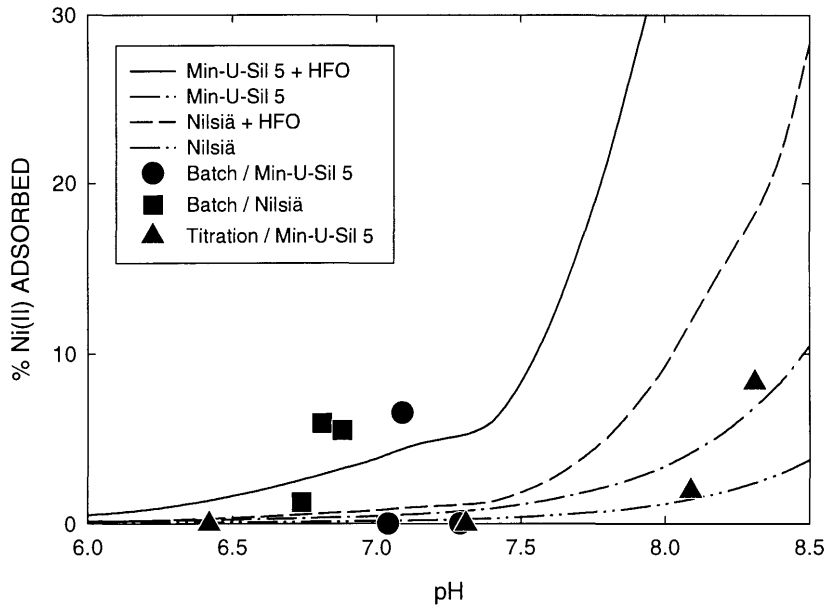

Figure 3 *Predicted (curves) vs. experimental (symbols) Ni(II) sorption on quartz in the saline groundwater simulant. For experimental data, consult Puukko and Hakanen (1997).*

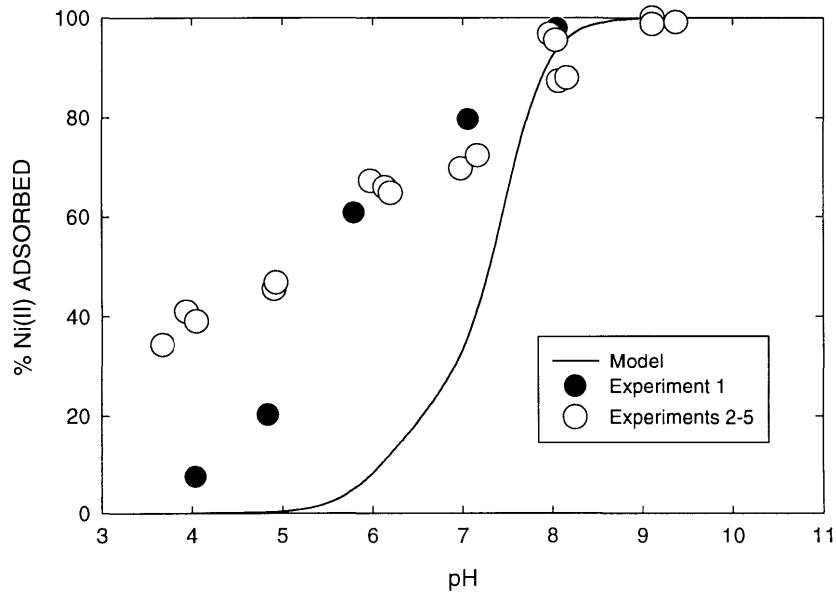

Figure 4. *Predicted (curve) and experimental (symbols) Ni(II) sorption on kaolinite in 0.001 M* $NaNO_3$.

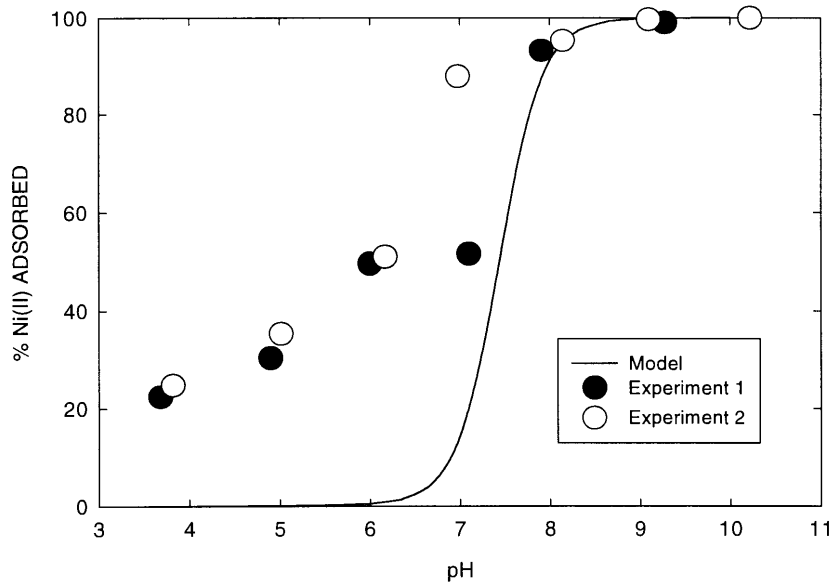

Figure 5. *Predicted (curve) and experimental (symbols) Ni(II) sorption on kaolinite in 0.01 M $NaNO_3$.*

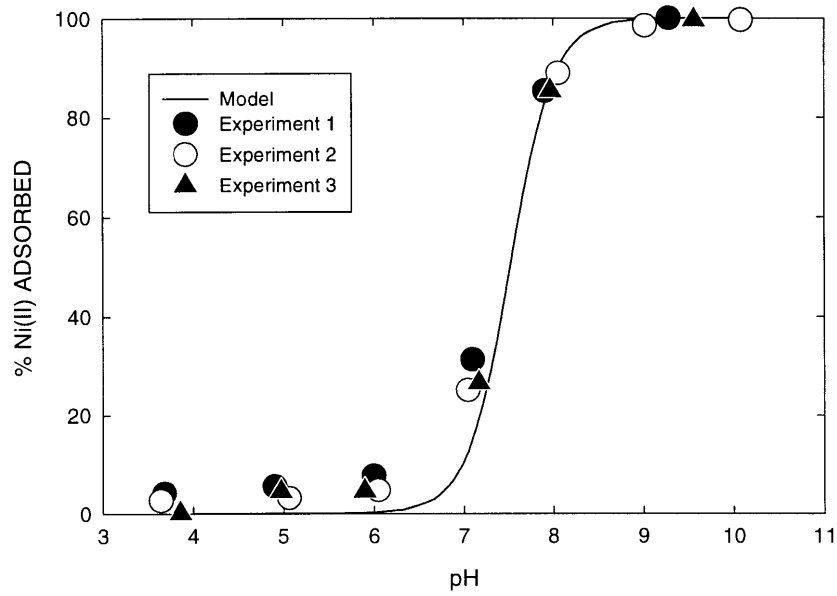

Figure 6. *Predicted (curve) and experimental (symbols) Ni(II) sorption on kaolinite in 0.1 M $NaNO_3$.*

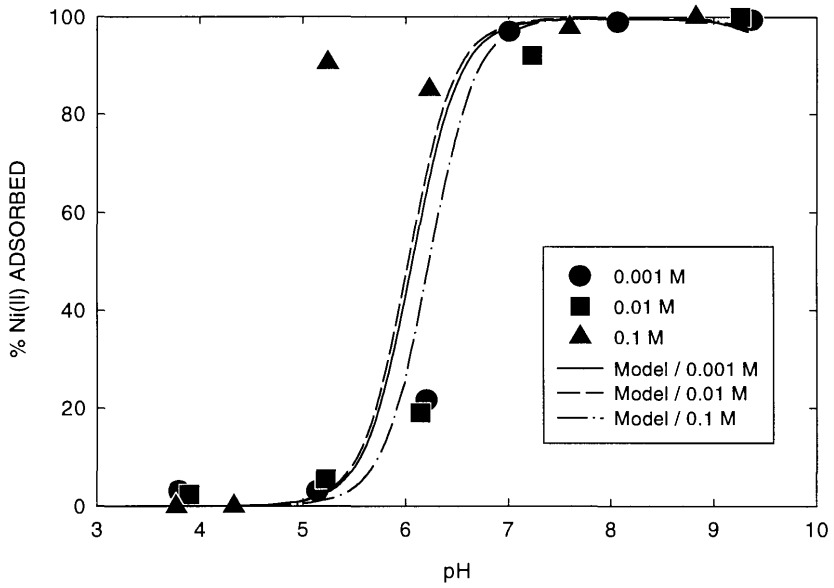

Figure 7. *Predicted (curves) vs. experimental (symbols) Ni(II) sorption on goethite in 0.001 M–0.1 M* $NaNO_3$.

2.3.5 Thorium on quartz

Because thorium, Th(IV), was not considered in our previous report, aqueous speciation and solubility were also studied. The results are shown in Figure 8. The solubility was limited by the amorphous phase, because the formation of the crystalline phase, thorianite, was assumed to be slow in laboratory conditions; if the crystalline phase is chosen, the solubility is much lower, as shown in Figure 9. The predicted sorption curve is shown in Figure 10 together with the experimental results.

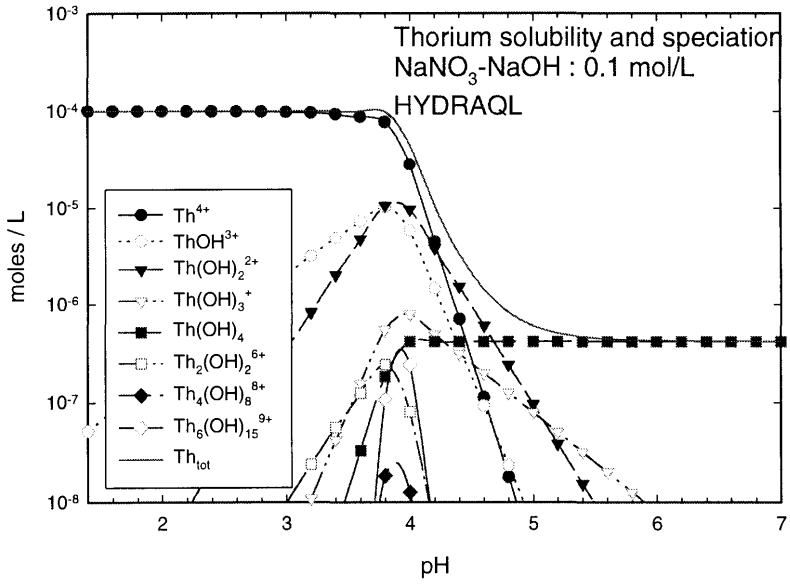

Figure 8. Th(IV) aqueous speciation. Tetravalent ion is dominant at low pH values while the neutral species is dominant at higher pH values, where the lowest solubility is reached, giving a concentration of about 0.4 µmol/L.

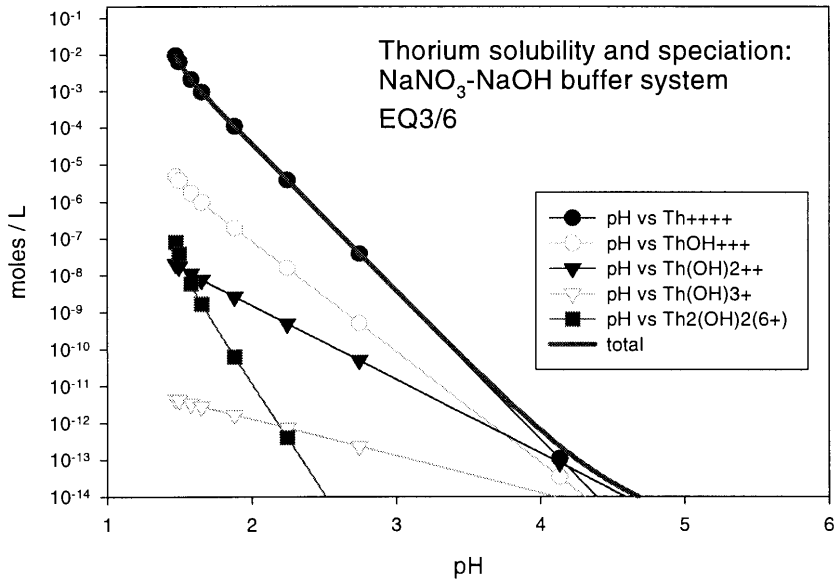

Figure 9. *Th(IV) solubility by EQ3/6 assuming the formation of thorianite.*

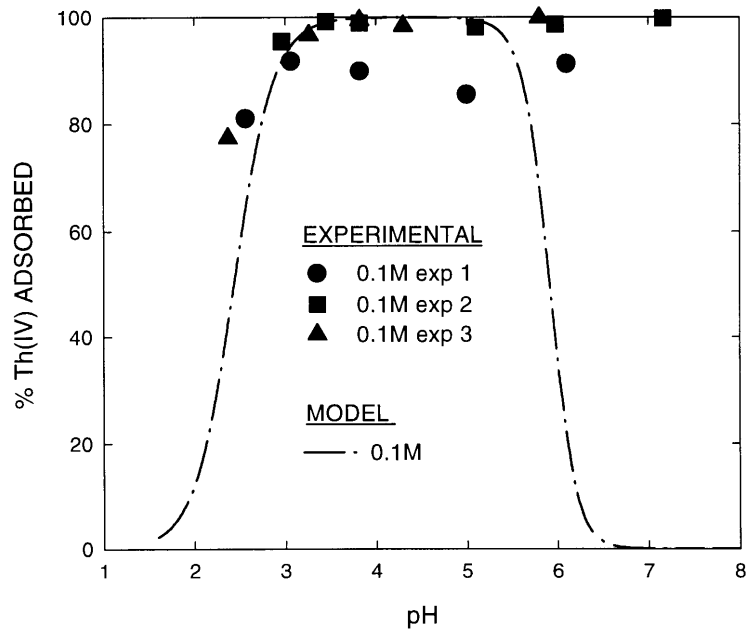

Figure 10. *Predicted Th(IV) sorption on quartz.*

3 MODELLING RESULTS

3.1 NICKEL ON A MIXTURE OF QUARTZ AND MnO_2

In our previous study (Olin, 1995), we assumed that small amounts of manganese dioxide may explain the observed high sorption of nickel on quartz at low pH values and at low ionic strength. The analysed Mn concentration was too low (less than 3.2 µg per gram of SiO_2) to cause any noticeable sorption. Nevertheless, it was decided to carry out some additional experiments with manganese. The experiments are described in more detail in Puukko and Hakanen (1997), and the results are shown in Figure 11.

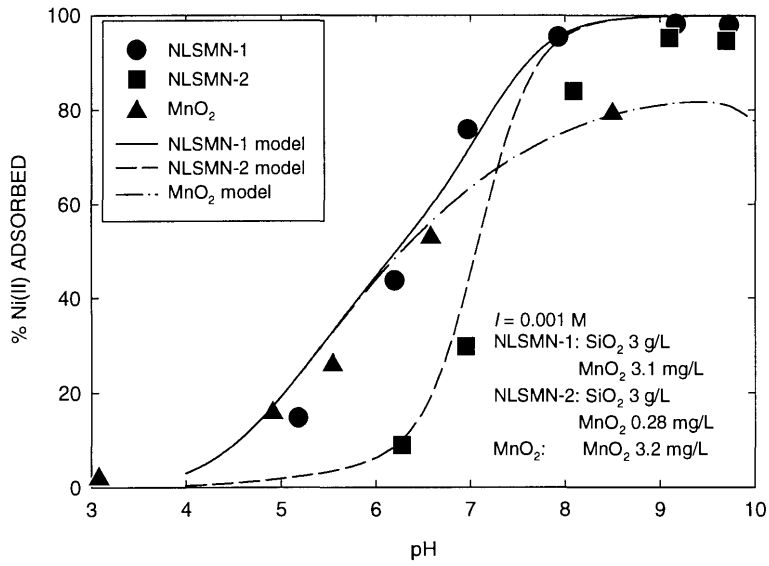

Figure 11. *Sorption of nickel on a mixture of quartz and MnO_2 in 0.001 M $NaNO_3$ was modelled using the data shown in Tables 9 and 10. The results depict the dominance of manganese dioxide in the acid and near-neutral region.*

3.2 NICKEL ON QUARTZ IN SYNTHETIC GROUNDWATER

In the preliminary modelling stage, the sorption results from experiments carried out by Puukko and Hakanen (1997) were best explained by assuming that HFO acts as an auxiliary adsorbent (Figures 2 and 3). Without the introduction of HFO, the predicted adsorption curves become greatly underestimated. According to the results shown in Figures 2 and 3, Ni(II) adsorbs appreciably less in the saline simulant due to the increased metal-metal competition for sorption sites compared to the fresh water. It should be borne in mind, however, that the modelling results are constrained by the presumption that there is no nickel species complexation with carbonate species. Furthermore, the set of binding constants in Table 6 is not consistent.

Next we tried to model the sorption of Ni(II) on quartz by using the data estimated from theoretical considerations and known properties of the solid by Sverjensky (1993) and Sverjensky and Sahai (1996). Had the binding constant for Ni(II),

given in Sverjensky (1993), been used, the predicted sorption would become over-estimated. Therefore, our strategy was to vary the binding constant until a good fit to the experimental data for Min-U-Sil 5 quartz in the fresh-water simulant was attained. The resulting subset of parameters and sorption constants are presented in Tables 9 and 10. The rest of the data are as given in Tables 5 and 6.

Table 9. *TLM parameters for quartz.*

Parameter	Value
Inner-layer capacitance, C_1	1.1 F/m^2
Site density, N_s	2.31 sites/nm^2

Table 10. *Surface chemical reactions (TLM) for quartz.*

Surface reaction	log K
Inner-sphere	
$SiOH + H^+ = SiOH_2^+$	-1.1†
$SiOH = SiO^- + H^+$	-7.1†
Outer-sphere	
$SiOH + Ni^{2+} = NiO^- - Ni^{2+} + H^+$	-3.65

† Sverjensky and Sahai (1996).

The results from HYDRAQL runs are shown in Figures 12 and 13 for the fresh and saline simulants respectively. The main conclusion here is that using the data in Tables 9 and 10, no adsorbents other than quartz are needed to explain nickel sorption. However, one point that obviously warrants further attention is the in-consistency of the data used.

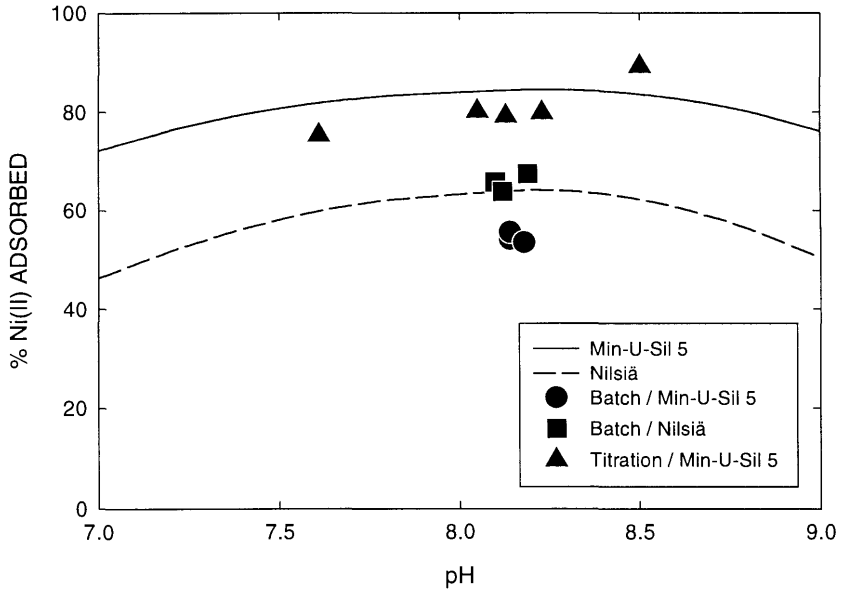

Figure 12. *Predicted (curves) vs. experimental (symbols) Ni(II) sorption on quartz in the fresh groundwater simulant.*

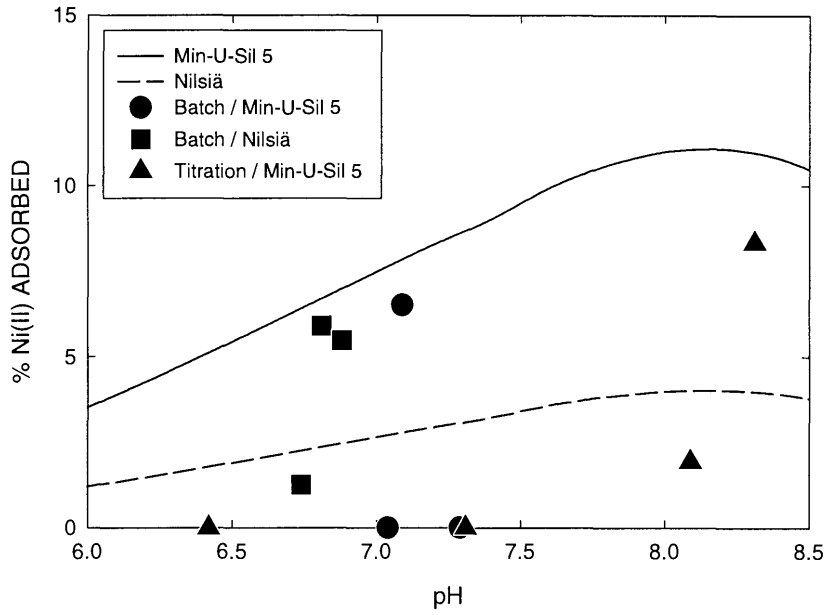

Figure 13. *Predicted (curves) vs. experimental (symbols) Ni(II) sorption on quartz in the saline groundwater simulant.*

3.3 NICKEL ON KAOLINITE

From Figures 4 and 5, it can be seen that the model-fit in 0.001 M and 0.01 M $NaNO_3$ background especially at low pH, respectively, is far from being adequate. It would appear that the cation-exchange capacity (CEC) of KGa-1 is actually much higher than that assumed in this work, 2 meq/100 g (the small kink in Figure 4 at pH 5.5–7 might be due to the cation-exchange contribution). In terms of isomorphous substitution in the clay crystal lattice, this typical value of the CEC suggests that one Si(IV) out of 400 needs to be replaced by an Al(III) in the lattice (Spark *et al.*, 1995). It is somewhat uncertain as to how much substitution in "well-crystallized" KGa-1 kaolinite could take place to give rise to a pH-independent charge. One source of the CEC in kaolins might be smectite impurities. However, KGa-1 is a relatively pure Georgia kaolin; its main mineralogical impurities include 1.7% anatase (TiO_2), 0.02% Fe oxides, 0.1% micas, and trace quartz (Brady *et al.*, 1996). In this light, the CEC of 2 meq/100 g seems reasonable enough. Chorom and Rengasamy (1995) found that the <2 μm fraction of Georgia kaolinite contained about 5% smectite. Even this value is not high enough to quantify the adsorption tendency shown in Figures 4 and 5. It was somewhat unclear if the material they used was KGa-1 or "poorly crystallized" KGa-2. Schindler *et al.* (1987) and Zachara *et al.* (1992) found behaviour similar to that in Figure 5 for Cu(II), Cd(II) and Pb(II) adsorption on KGa-1 in the acid region in 0.01 M $NaClO_4$ background media. Encouraged by this, we applied Schindler *et al.*'s set of data for Cd(II) and Pb(II) to the present system, but were not able to improve the fit. Brady *et al.* (1996) concluded that the Al sites at the kaolinite surface are appreciably more acidic than in its component oxide (see also Spark *et al.* (1995b)). Led by this and the idea that the gibbsite-like basal faces of kaolinite are

ionizable in aqueous media (e.g., Zhou and Gunter, 1992), Brady *et al.* (1996) modelled surface charge development by assuming the surface reaction to occur equivalently on edges and basal planes, and by assuming the structural permanent charge negligibly small. Using Brady *et al.*'s set of surface ionization data (CCM) and the binding constants for Ni(II) in Table 8 (the resulting data set is inconsistent, however), no significant improvement was obtained. This may, in part, be due to the fact that Brady *et al.* (1996) used a background electrolyte concentration high enough (0.1 M NaCl) to suppress the potential contribution of exchange sorption. Lastly, we tried to model Ni(II) adsorption on kaolinite using Sverjensky's approach (see section 3.1). The relevant set of parameters and equilibrium constants (TLM) are given in Tables 11 and 12 respectively.

Table 11. *TLM parameters for kaolinite (Sverjensky and Sahai, 1996).*

Parameter	Value
Specific surface area, S	11.38 $m^2/g^{\dagger}$
Inner-layer capacitance, C_1	1.4 $F/m^{2\ddagger}$
Outer-layer capacitance, C_2	0.2 F/m^2
Site density, N_s	2.31 sites/nm^2

† Puukko and Hakanen (1997).
‡ From Figure 10 in Sverjensky and Sahai (1996).

Table 12. *Surface chemical reactions (TLM) for kaolinite.*

Surface reaction	log K
Inner-sphere	
$SOH + H^+ = SOH_2^+$	$1.1^{\dagger}$
$SOH = SO^- + H^+$	$-8.2^{\dagger}$
Outer-sphere	
$SOH + Ni^{2+} = SO^- - Ni^{2+} + H^+$	$-2.2^{\ddagger}$

† Sverjensky and Sahai (1996).
‡ Calculated from the product of the binding constants for the reactions $SO^- + Ni^{2+} = SO^- - Ni^{2+}$ (Sverjensky, 1993) and $SOH = SO^- + H^+$.

The modelling results are depicted in Figures 14 to 16. As can be seen from these figures, the model sorption curves have shifted to the left and no improvement over the preliminary modelling results was obtained.

A plausible explanation for the unexpectedly high sorption at acidic pH is mineral dissolution followed by re-adsorption or precipitation of Al on the mineral surface, which alters the sorptive properties of kaolinite (Schroth and Sposito, 1997). Also, the fact that these authors determined the CEC of KGa-1 to be 0.63 meq/100 g supports the hypothesis that the high uptake of Ni(II) at low pH is an experimental artefact rather than adsorption on an unaltered kaolinite specimen.

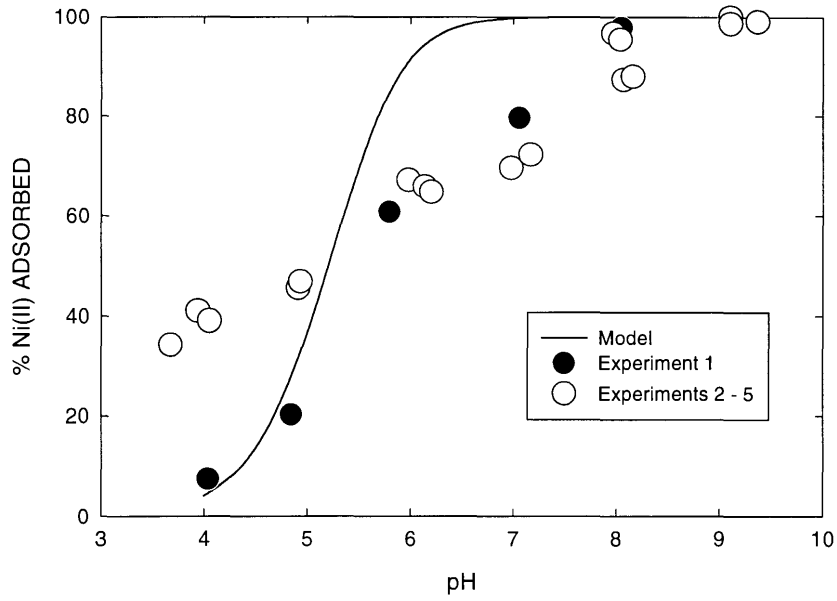

Figure 14. *Predicted (curve) and experimental (symbols) Ni(II) sorption on kaolinite in 0.001 M $NaNO_3$.*

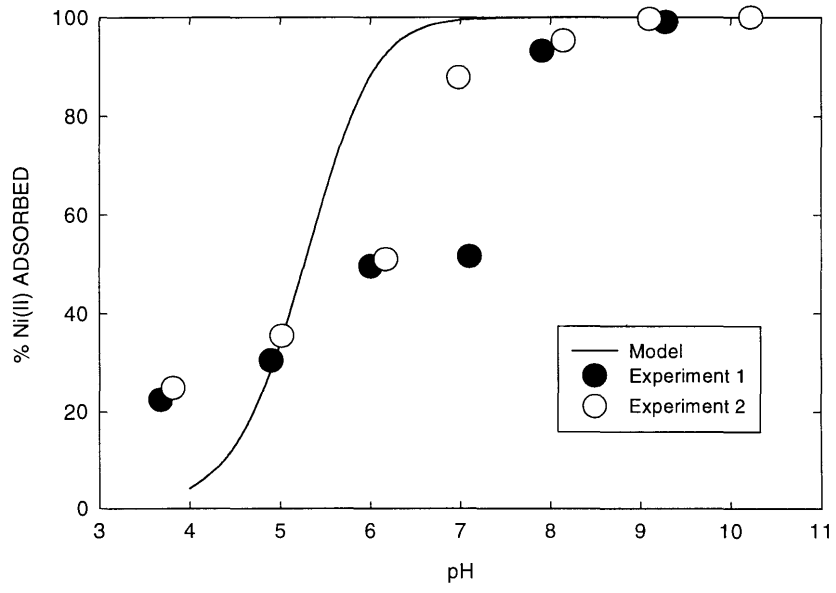

Figure 15. *Predicted (curve) and experimental (symbols) Ni(II) sorption on kaolinite in 0.01 M $NaNO_3$.*

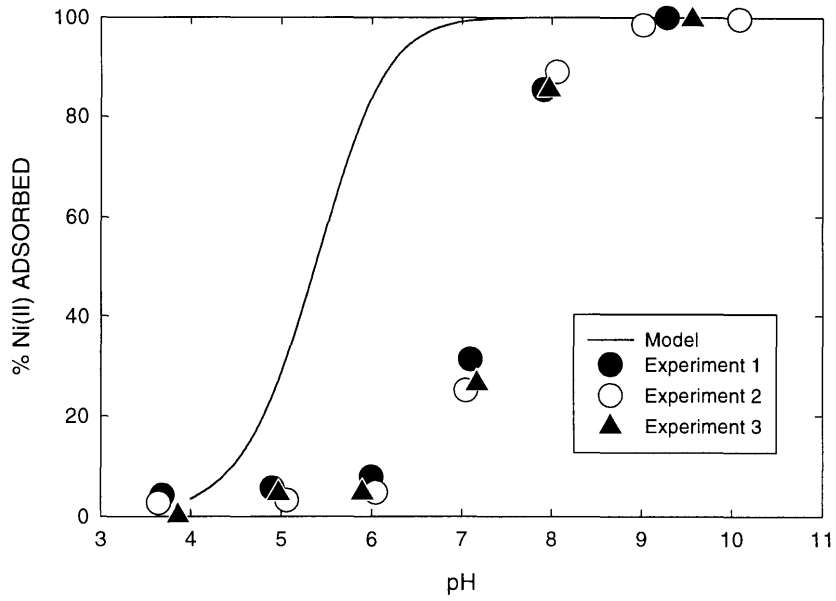

Figure 16. *Predicted (curve) and experimental (symbols) Ni(II) sorption on kaolinite in 0.1 M* $NaNO_3$.

3.4 NICKEL ON GOETHITE

The modelled sorption results as a function of pH for 0.001 M–0.1 M $NaNO_3$ are depicted in Figure 7. Except for one experimental point for 0.1 M $NaNO_3$ at pH ~5, the fit is very good. Due to the (postulated) inner-sphere surface complexation of Ni(II), variations in the ionic strength of $NaNO_3$ do not significantly affect nickel adsorption. This view is also supported by the experimental results of Spark *et al.* (1995a) for trace metal sorption on goethite in KNO_3 background media.

3.5 THORIUM ON QUARTZ

The results from speciation calculations are shown in Figure 17. The neutral species becomes dominant after pH 5, the sorption probably being low at pH higher than 5. The ionic strength, 0.1 M, was chosen high enough to be realistic at pH less than 2, which was needed for sorption studies.

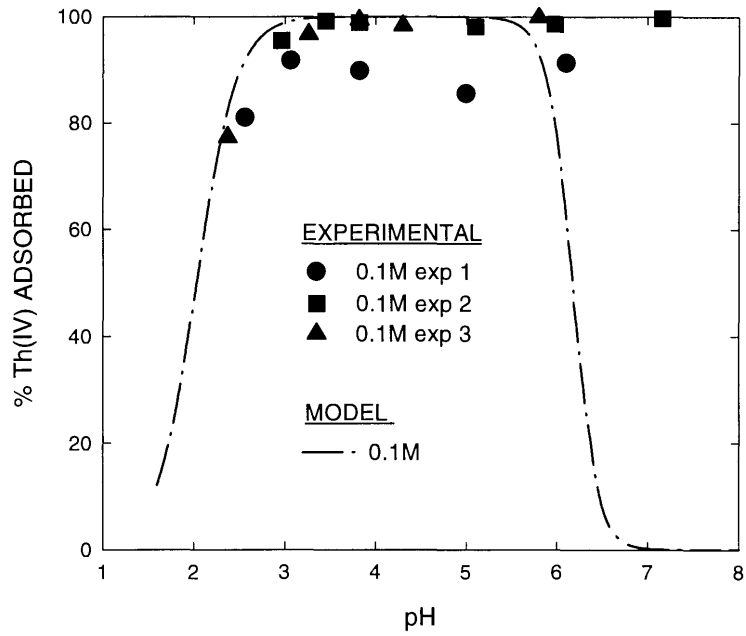

Figure 17. *Thorium(IV) sorption on quartz was modelled by modifying the binding constant for thorium due to Östhols' use of different aqueous data.*

4 CONCLUSIONS

The mechanistic sorption models provide a tool for interpreting the sorption processes. This interpretation is easy to check by predicting experimental results using some existing literature data and measuring the sample-specific parameters (e.g., the amount of adsorbent), and comparing the calculated and measured sorption values. The success of such predictions gives valuable information about uncertainties in K_d-values, which are the relevant parameters in safety assessment studies.

In this investigation, surface complexation modelling was applied to nickel sorption on quartz, goethite and kaolinite, and thorium sorption on quartz. Goethite was somewhat straightforward to model. The tendency for nickel(II) to form inner-sphere complexes with the goethite surface was indirectly verified. As to the kaolinite, more experimental and modelling effort, especially at low pH is obviously needed. This would include, for example, a careful analysis of the pH-independent cation-exchange capacity (if any) arising from substitutions in the clay structure and the quality of sorption data. A satisfactory prediction for the mixture of quartz and MnO_2 was obtained. No particular problems with thorium sorption were encountered. However, it was not possible to experimentally verify the bending of the predicted sorption curve in the near-neutral region.

One point that deserves attention and applies to most systems under study is that a great deal of difficulties arise either from the complete lack of sorption data or from its inconsistency, or both.

REFERENCES

Balistrieri, L. S., and Murray, J. W. 1982. The surface chemistry of δMnO_2 in major ion seawater. *Geochim. Cosmochim. Acta,* **46**, 1041-1052.

Bansal, O. P. 1982. Thermodynamics of K-Ni and Ca-Ni exchange reactions on kaolinite clay. *J. Soil Sci.*, **33**, 63-71.

Brady, P. V., Cygan, R. T., and Nagy, K. L. 1996. Molecular controls on kaolinite surface charge. *J. Colloid Interface Sci.*, **183**,. 356-364.

Chorom, M., and Rengasamy, P. 1995. Dispersion and zeta potential of pure clays as related to net particle charge under varying pH, electrolyte concentration and cation type. *European J. Soil Sci.*, **46**, 657-665.

Coughlin, B. R., and Stone, A. T. 1995. Nonreversible adsorption of divalent metal ions (Mn^{II}, Co^{II}, Ni^{II}, Cu^{II}, and Pb^{II}) onto goethite: Effects of acidification, Fe^{II} addition, and picolinic acid addition. *Environ. Sci. Tech.*, **29**, 2445-2455.

Davies, C. W. 1962. Ion association. London, Butterworths. 190 p.

Dzombak, D. A., and Morel, F. M. M. 1990. Surface complexation modelling: hydrous ferrous oxide. John Wiley & Sons, New York. 393 p.

Ewin, G. J., Erno, B. P., and Hepler, L. G. 1981. Clay chemistry: Investigation of ion exchange reactions by titration calorimetry, *Can. J. Chem.*, **59**, 2927-2933.

Goldberg, S. 1993. Constant capacitance model: Chemical surface complexation model for describing adsorption of toxic trace elements on soil minerals. In: D. W. Tedder, and F. G. Pohland (eds.), Emerging Technologies in Hazardous Waste Management III, Am. Chem. Soc. Symp. Ser. 518, pp. 278-307.

Kent, D. B., Tripathi, V. S., Ball, N. B., and Leckie, J. O. 1986. Surface complexation modeling of radionuclide adsorption in sub-surface environments, Technical Report No. 294, Dept. of Civil Engineering, Stanford University, California, 110 p.

Leckie, J. O. 1995. Ternary complex formation at mineral/solution interfaces. In: Binding models concerning natural organic substances in performance assessment, OECD/NEA, pp. 181-212.

Olin, M. 1995. Surface complexation modelling applied to the sorption of nickel on silica. Helsinki, Nuclear Waste Commission of Finnish Power Companies, Report YJT-95-10. 47 p.

Papelis, C., Hayes, K. F., and Leckie, J. O. 1988. HYDRAQL: A program for the computation of chemical equilibrium composition of aqueous batch systems including surface-complexation modeling of ion adsorption at the oxide/solution interface: Technical report number 306, Department of Civil Engineering, Stanford University, Stanford, California, 130 p.

Payne, T. E., and Waite, T. D. 1991. Surface complexation modelling of uranium sorption data obtained by isotope exchange techniques. *Radiochim. Acta*, **52/53**, 487-493.

Puukko, E., and Hakanen, M. 1995. Surface complexation modelling: experiments on the sorption of nickel on quartz. Helsinki, Nuclear Waste Commission of Finnish Power Companies, Report YJT-95-12. 20 p.

Puukko, E., and Hakanen, M. 1997. Surface complexation modelling: experiments on sorption of nickel on quartz, goethite, and kaolinite and preliminary results on sorption of thorium on quartz. Report Posiva 97-06. 34 p.

Schindler, P. W. 1991. A solution chemist's view of surface chemistry. *Pure & Appl. Chem.*, **63**, 1697-1704.

Schindler, P. W., and Sposito, G. 1991. Surface complexation at (hydr)oxide surfaces. In: Bolt, G. H., De Boodt, M. F., Hayes, M. H. B., and McBride, M. B. (eds.), Interactions at the Soil Colloid - Soil Solution Interface, Kluwer Academic Publishers, pp. 115-145.

Schindler, P. W., Liechti, P., and Westall, J. C. 1987. Adsorption of copper, cadmium and lead from aqueous solution to the kaolinite/water interface. *Netherlands J. Agric. Sci.*, **35**, 219-230.

Schroth, B. K., and Sposito, G. 1997. Surface charge properties of kaolinite. *Clays and Clay Minerals*, **45**, 85-91.

Spark, K. M., Johnson, B. B., and Wells, J. D. 1995a. Characterizing heavy-metal adsorption on oxides and oxyhydroxides. *European J. Soil Sci.*, **46**, 621-631.

Spark, K. M., Wells, J. D., and Johnson, B. B. 1995b. Characterizing trace metal adsorption on kaolinite. *European J. Soil Sci.*, **46**, 633-640.

Sverjensky, D. A. 1993. Physical surface-complexation models for sorption at the mineral-water interface. *Nature*, **364**, 776-780.

Sverjensky, D. A., and Sahai, N. 1996. Theoretical prediction of single-site surface protonation equilibrium constants for oxides and silicates in water. *Geochim. Cosmochim. Acta,* **60**, 3773-3797.

White, G. N., and Zelazny, L. W. 1988. Analysis and implications of the edge structure of dioctahedral phyllosilicates. *Clays and Clay Minerals*, **36**, 141-146.

Wolery, T. J. 1992. EQ3/6, A software package for geochemical modeling of aqueous systems: Package overview and installation guide (Version 7.0). California, Lawrence Livermore National Laboratory, Report UCRL-MA-110662 PT I. 66 p.

Xie, Z., and Walther, J. V. 1992. Incongruent dissolution and surface area of kaolinite. *Geochim. Cosmochim. Acta*, **56**, 3357-3363.

Zachara, J. M., Ainsworth, C. C., Cowan, C. E., and Schmidt, R. L. 1990. Sorption of aminonaphtalene and quinoline on amorphous silica. *Environ. Sci. Technol.*, **24**, 118-126.

Zachara, J. M., Smith, S. C., Resch, C. T., and Cowan, C. E. 1992. Cadmium sorption to soil separates containing layer silicates and iron and aluminum oxides. *Soil Sci. Soc. Am. J.*, **56**, 1074-1084.

Zhou, Z., and Gunter, W. D. 1992. The nature of the surface charge of kaolinite. *Clays and Clay Minerals*, **40**, 365-368.

Östhols, E. 1995. Thorium sorption on amorphous silica. *Geochim. Cosmochim. Acta*, **59**, 1235-1249.

LIST OF POSIVA REPORTS 1997, situation 12/97

POSIVA-97-01
Model for diffusion and porewater chemistry in compacted bentonite
Theoretical basis and the solution methodology for the transport model
Jarmo Lehikoinen
VTT Chemical Technology
January 1997
ISBN 951-652-026-X

POSIVA-97-02
Model for diffusion and porewater chemistry in compacted bentonite
Experimental arrangements and preliminary results of the porewater chemistry studies
Arto Muurinen, Jarmo Lehikoinen
VTT Chemical Technology
January 1997
ISBN 951-652-027-8

POSIVA-97-03
Comparison of 3-D geological and geophysical investigation methods in boreholes KI-KR1 at Äänekoski Kivetty site and RO-KR3 at Kuhmo Romuvaara site
Katriina Labbas
Helsinki University of Technology
Material Science and Rock Engineering
January 1997
ISBN 951-652-028-6

POSIVA-97-04
Summary Report - Development of Laboratory Tests and the Stress-Strain Behaviour of Olkiluoto Mica Gneiss
Matti Hakala, Esa Heikkilä
Laboratory of Rock Engineering
Helsinki University of Technology
May 1997
ISBN 951-652-029-4

POSIVA-97-05
Radionuclide solubilities at elevated temperatures - a literature study
Torbjörn Carlsson, Ulla Vuorinen
Technical Research Centre of Finland
July 1997
ISBN 951-652-030-8

POSIVA-97-06
Surface complexation modelling: Experiments on sorption of nickel on quartz, goethite and kaolinite and preliminary tests on sorption of thorium on quartz
Esa Puukko, Martti Hakanen
University of Helsinki
Department of Chemistry
Radiochemistry laboratory
September 1997
ISBN 951-652-031-6

POSIVA-97-07

Diffusion and sorption of HTO, Np, Na and Cl in rocks and minerals of Kivetty and Olkiluoto
Vesa Kaukonen, Martti Hakanen
University of Helsinki
Department of Chemistry
Laboratory of Radiochemistry
Antero Lindberg
Geological Survey of Finland
October 1997
ISBN 951-652-032-4

POSIVA-97-08

Regression methodology in groundwater composition estimation with composition predictions for Romuvaara borehole KR10
Ari Luukkonen, Juhani Korkealaakso, Petteri Pitkänen
VTT Communities and Infrastructure
November 1997
ISBN 951-652-033-2

POSIVA 97-09

Dissolution of unirradiated UO_2 fuel in synthetic saline groundwater - Experimental methods and preliminary results
Kaija Ollila
VTT Chemical Technology
December 1997
ISBN 951-652-034-0

POSIVA 97-10

Application of surface complexation modelling: Nickel sorption on quartz, manganese oxide, kaolinite and goethite and thorium on silica
Markus Olin, Jarmo Lehikoinen
VTT Chemical Technology
December 1997
ISBN 951-652-035-9